Supporting Information

Spontaneous Si-C Bond Cleavage in (Triphos^{Si})-Nickel Complexes

Anette Petuker,[a] Stefan Mebs,[b] Nils Schuth,[b] Philipp Gerschel,[a] Matthew L. Reback,[a] Bert Mallick,[a] Maurice van Gastel,*[c] Michael Haumann,*[b] and Ulf-Peter Apfel*[a]

[a] Ruhr University Bochum, Inorganic Chemistry I, Universitätsstraße 150, 44801 Bochum.

[b] Freie Universität Berlin, Department of Physics, Arnimallee 14, 14195 Berlin.

[c] Max-Planck-Institut für chemische Energiekonversion, Stiftstrasse 34-36, 45470 Mülheim a. d. Ruhr.

Content

Figure S1 Structural motif of compound **3b(ClO_4)** 3

Figure S2 UV-vis spectra of compounds **3a(ClO_4)**, **3a(BF_4)** and **3b(ClO_4)** 3

Figure S3 UV-vis spectra of compounds **4** and **5** in Acetonitrile 4

Figure S4 UV-vis spectra of compound **5** in acetonitrile 4

Figure S5 ^{31}P NMR spectra of compound **1b**, complex **5** and reaction mixture of compound **1b** with $[Ni(CH_3CN)_6](BF_4)_2$ in MeCN-d_3**.** 5

Figure S6 ^{31}P NMR spectra of complex **5**, PMe_3 and reaction mixture of complex **5** + 1eq PMe_3 in MeCN-d_3. 5

Figure S7 Structural motif of compound **8** and **9** 6

Figure S8 UV-vis spectra of compounds **3a(ClO_4)**, **5, 7a** and **7b** in THF 6

Figure S9 EPR spectrum of **7a** 7

Figure S10 Self-absorption correction of fluorescence-detected XAS spectra. 8

Figure S11 EXAFS analysis of Ni compounds 9

Figure S12 XANES spectra of Ni compounds 9

Figure S13 Kß X-ray emission spectra of Ni compounds 10

Figure S14 Nickel and ligand characters of ctv and vtc electronic transitions 11

Figure S15 Ni(d) orbital degeneracy. 12

Figure S16 Charge and spin density distribution 12

Figure S17 ^{31}P NMR spectra of complex **5**, the reaction mixture of compound **1b** with $Ni(ClO_4)_2$ with NaF after 5 min and the reaction mixture of compound **1b** with $Ni(ClO_4)_2$ with NaF after 1 day in MeCN-d_3 13

Figure S18 ^{31}P NMR spectra of complex **5**, compound **1b** and the reaction mixture of compound **1b** with $NiCl_2$ with NaF after 1 day in MeCN-d_3. 13

Figure S19 ^{31}P NMR spectra of complex **5** compound **1b** and the reaction mixture of compound **1b** with $[Ni(CH_3CN)_6](BF_4)_2$ with Ag(OTf) in MeCN-d_3 14

Figure S20 Relaxed surface scan for Si-C bond cleavage in the coordination complex of Triphos^{Si} to two Ni^{2+} cations after nucleophilic attack at Si by F^- 14

Table S1 EXAFS fit parameters and nickel-ligand bond lengths 15

Table S2 Molecular energies for different spin states 15

Table S3 Crystal Data and Refinement Details for the Crystal Structure Analyses of Compounds **3a(BF_4)** and **3b(ClO_4)** 16

Table S4 Crystal Data and Refinement Details for the Crystal Structure Analyses of Compounds **4**, **5** and **7a** 17

Table S5 Crystal Data and Refinement Details for the Crystal Structure Analyses of Compounds **7b**, **8** and **9**. 18

Table S6 Cartesian coordinates [Å] of the coordination complex of Triphos^{Si} to two Ni^{2+} cations after nucleophilic attack of F^- at Si 19

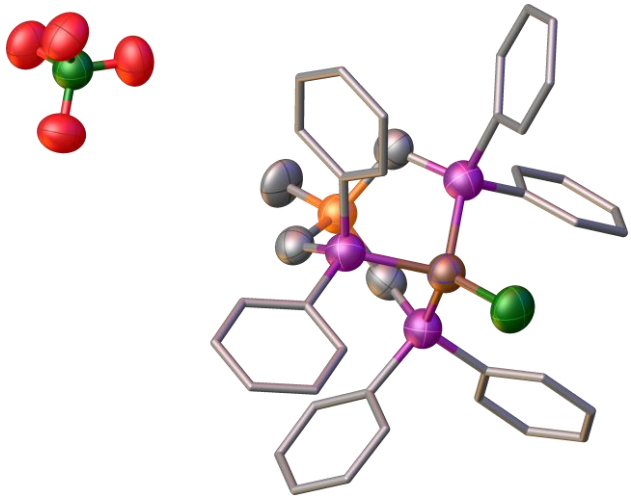

Figure S1 Structural motif of compound **3b(ClO$_4$)** with thermal ellipsoids at the 50% probability level (hydrogen atoms and thermal ellipsoids of phenyl groups were omitted for clarity).

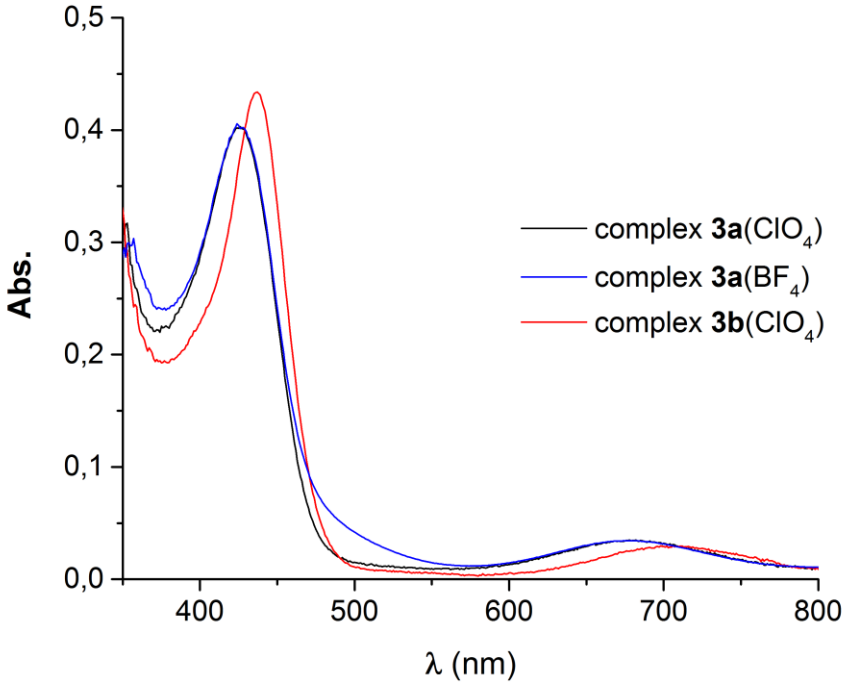

Figure S2 UV-vis spectra of compounds **3a(ClO$_4$)**, **3a(BF$_4$)** and **3b(ClO$_4$)** in THF.

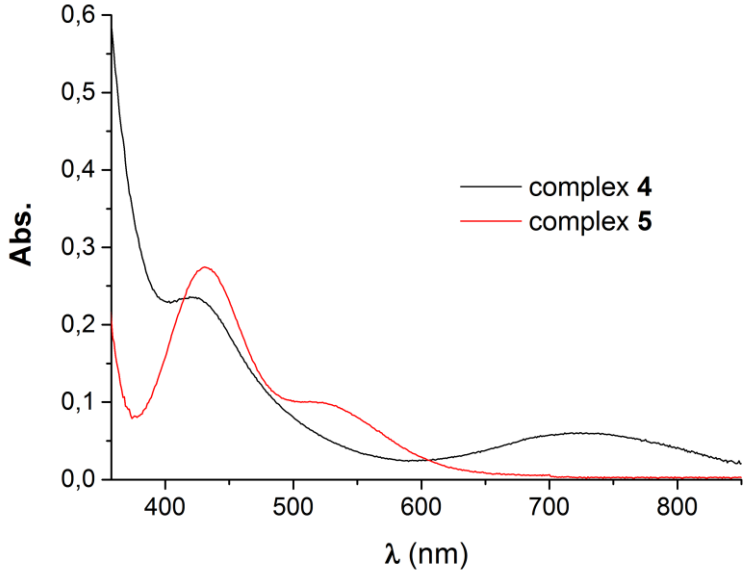

Figure S3 UV-vis spectra of compounds **4** and **5** in Acetonitrile.

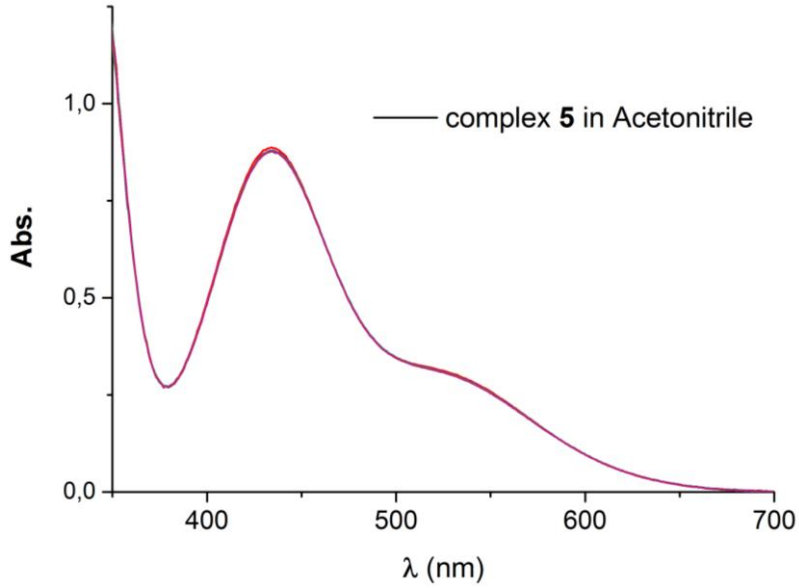

Figure S4 UV-vis spectra of compound **5** in acetonitrile. Measured over 60 min at 70°C.

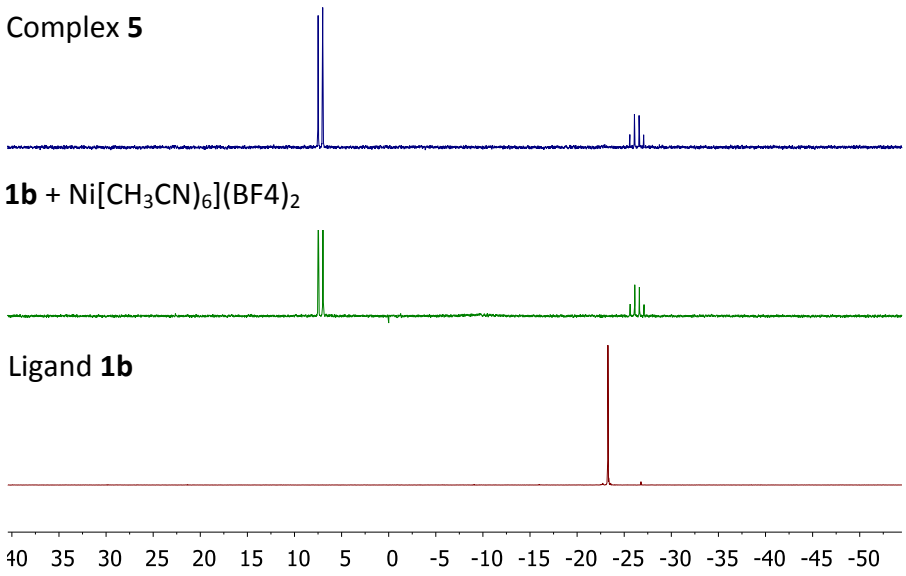

Figure S5 ^{31}P NMR spectra of compound **1b** (red line), complex **5** (blue line) and reaction mixture of compound **1b** with $[Ni(CH_3CN)_6](BF_4)_2$ in MeCN-d_3**.**

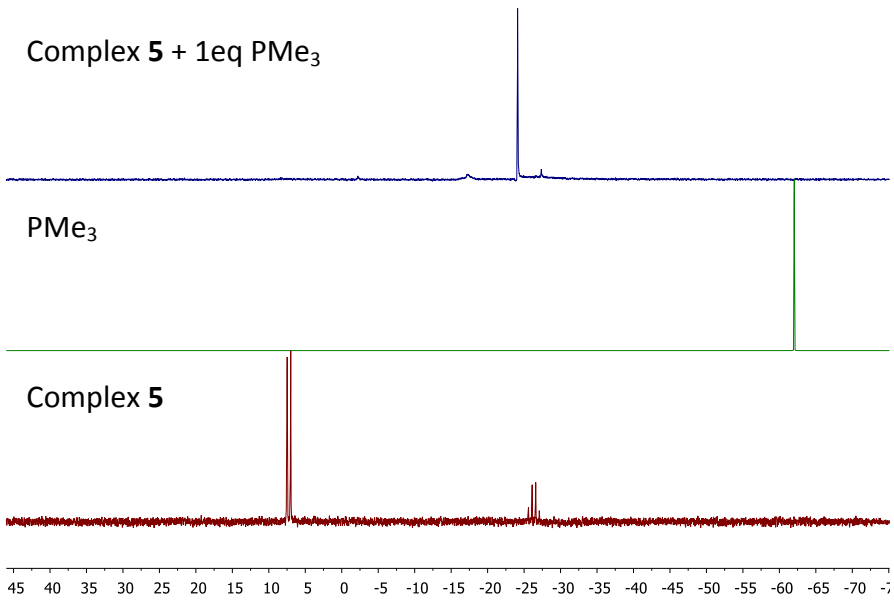

Figure S6 ^{31}P NMR spectra of complex **5** (red line), PMe_3 (green line) and reaction mixture of complex **5** + 1eq PMe_3 in MeCN-d_3 (blue line).

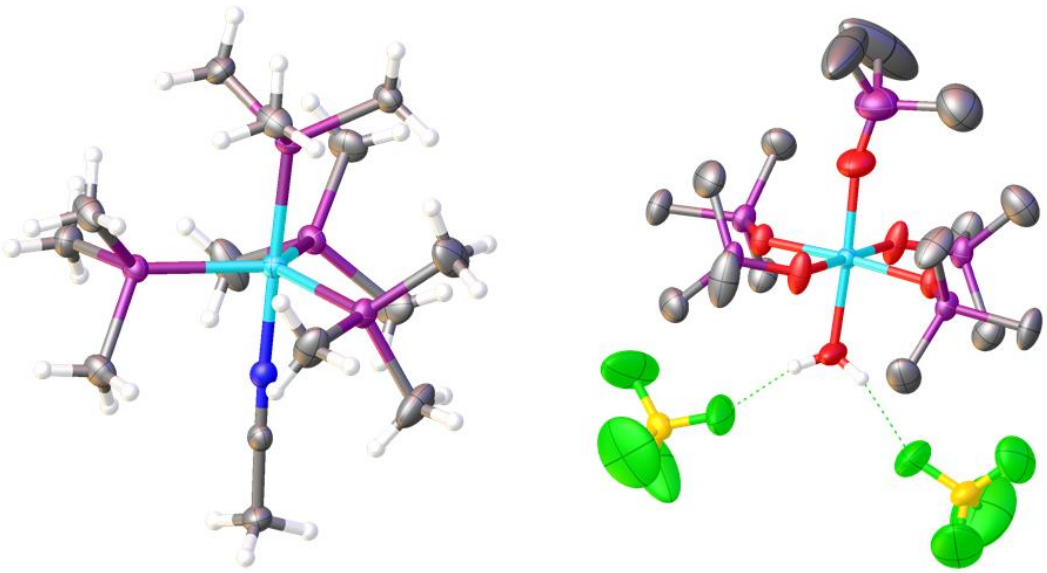

Figure S7 Structural motif of compound **8** (left) and **9** (right) with thermal ellipsoids at the 50% probability level (hydrogen atoms of compound **9** were omitted for clarity).

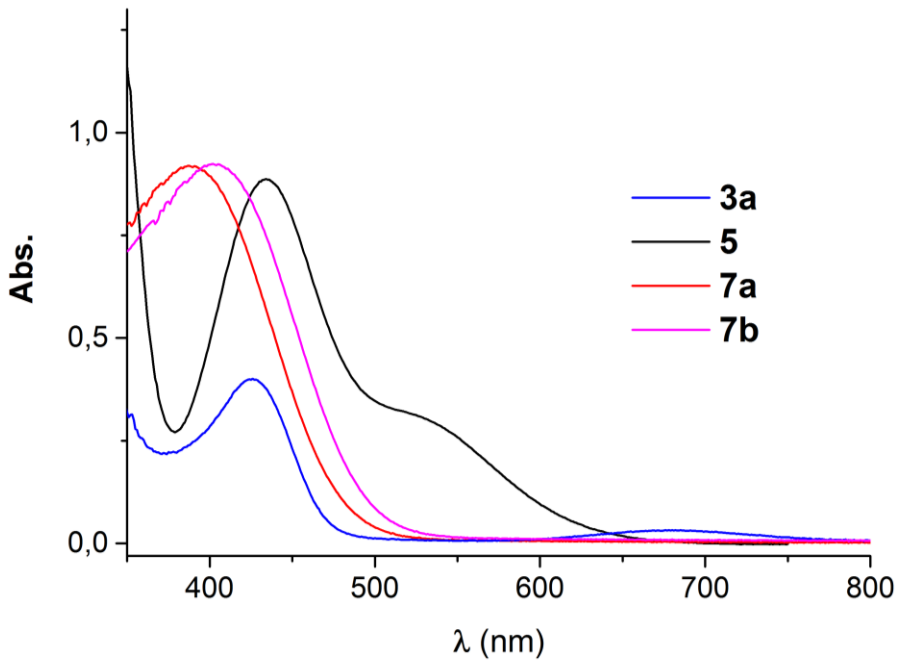

Figure S8 UV-vis spectra of compounds **3a(ClO_4)**, **5, 7a** and **7b** in THF.

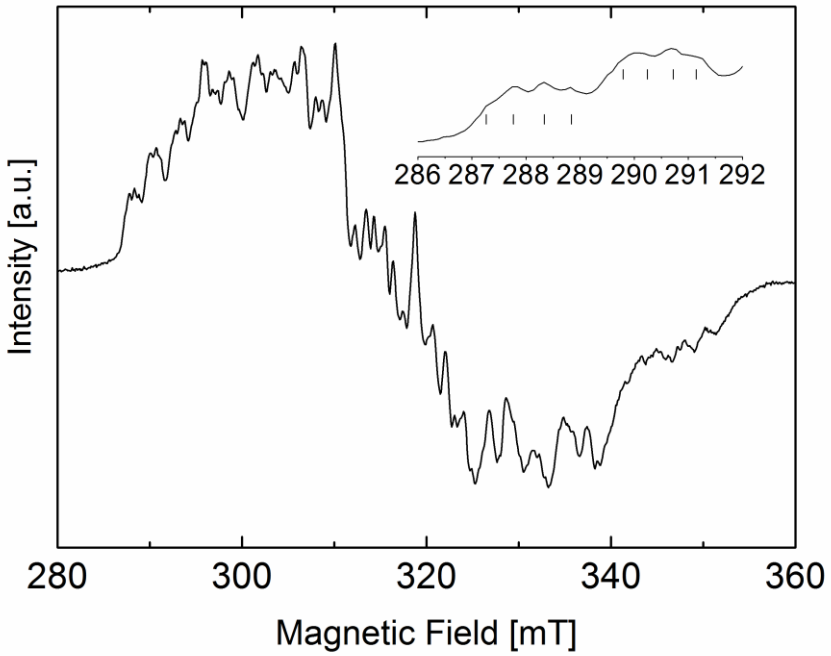

Figure S9. EPR spectrum of **7a**. The inset shows a zoom of the hyperfine structure with a pattern of 4 equidistant signals in 1:1:1:1 ratio, assigned to the chloride atom. Experimental conditions: T = 30K, frequency 9.65 GHz, microwave power 2mW, modulation amplitude 0.5 mT.

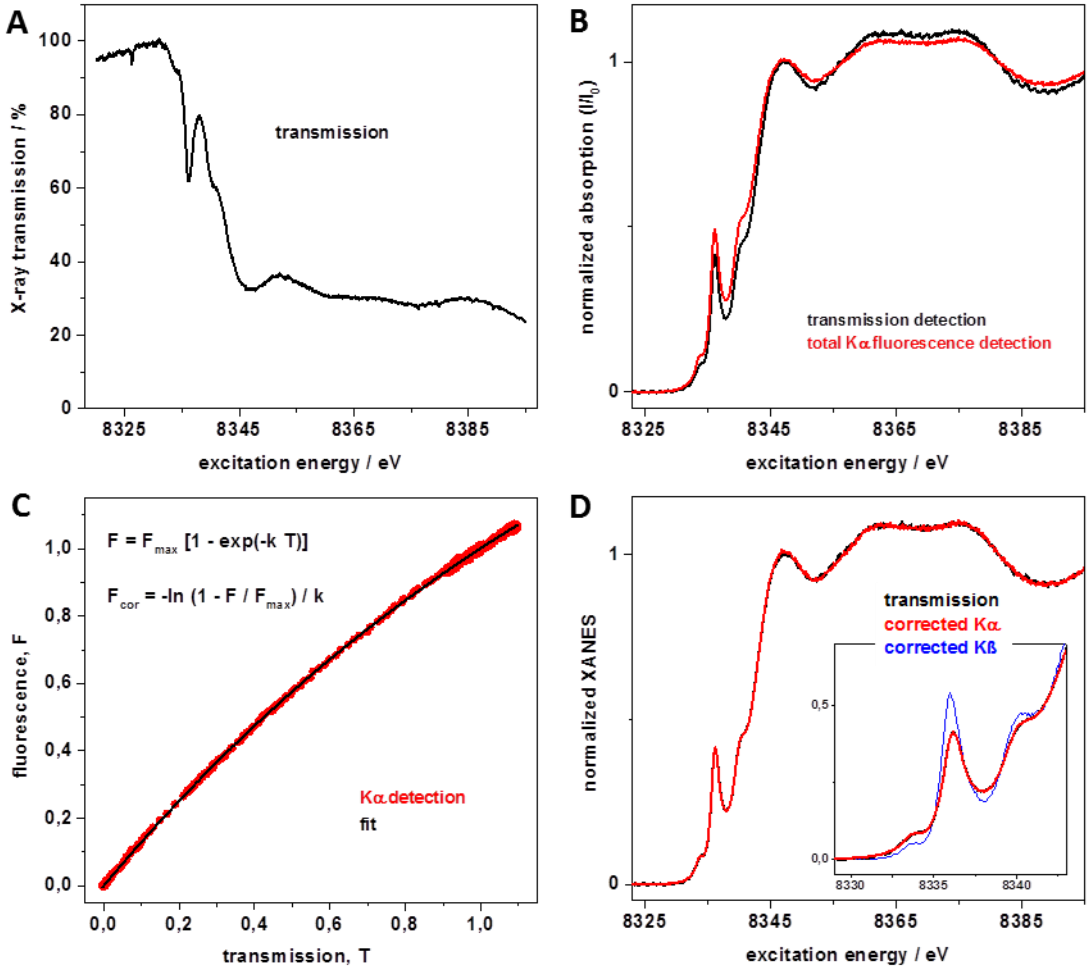

Figure S10 Self-absorption correction of fluorescence-detected XAS spectra. (A) Example of a raw transmission-detected K-edge spectrum of a concentrated powder sample of a nickel complex (**2a**) showing ~75 % absorption of incident X-rays above the edge jump (8345 eV). Transmission was set arbitrarily to 100 % before the edge jump (8330 eV). (B) Reabsorption of X-ray fluorescence photons (self-absorption) in the concentrated sample leads to increasing spectral flattening for increasing absorption and thereby causes relative enhancement of amplitudes of pre-edge features at low energies and damping of oscillations above the K-edge (EXAFS) in normalized Ka (or Kß) fluorescence-detected absorption spectra compared to the ("true") normalized transmission-detected spectrum. (C) Least-squares fitting of data points in a plot of fluorescence vs. transmission spectra by a saturation curve (top equation) yields parameters for correction of fluorescence-detected spectra (bottom equation). (D) The corrected Kα detected spectrum (F_{cor}) is identical to the transmission-detected spectrum in the whole XANES region and the narrow-band $K_ß$ detected spectrum (corrected using the same parameters as for the Ka-detected spectrum) in particular shows increased resolution of resonant transitions in the pre-edge region (inset).

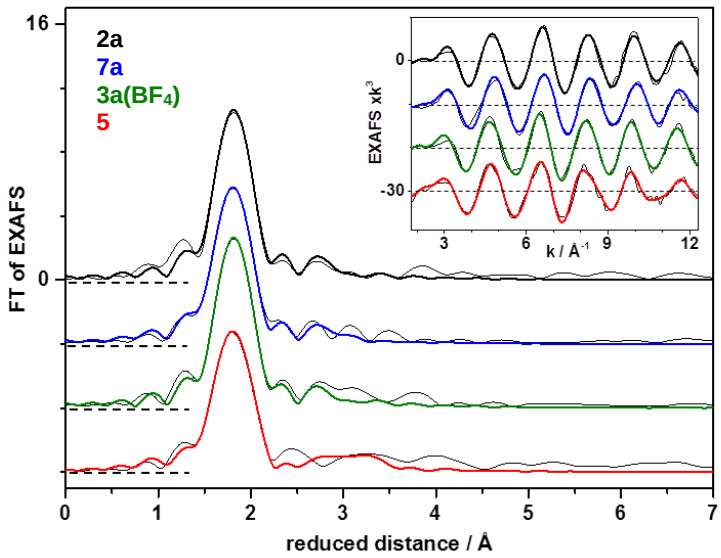

Figure S11 EXAFS analysis of Ni compounds. For the indicated nickel complexes, Fourier-transforms (FTs) of EXAFS oscillations in the inset were vertically shifted for comparison. Thin lines, experimental data; thick lines, simulations with parameters in Table S1. FTs were calculated for a *k*-range of 1.7-12.3 $Å^{-1}$ using cos windows extending over 10% at both *k*-range ends. Spectra were collected in absorption mode (transmission).

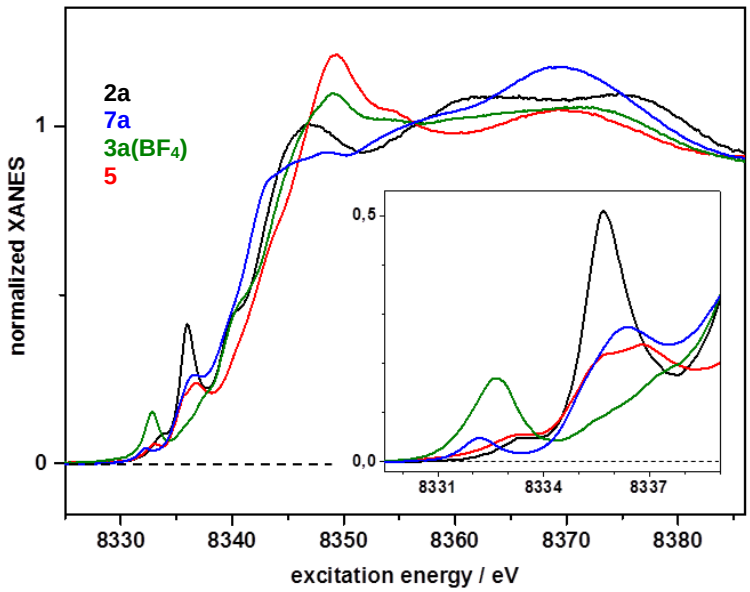

Figure S12 XANES spectra of Ni compounds. Main panel: absorption spectra of indicated compounds detected in transmission mode. Inset: pre-edge absorption spectra at increased resolution from narrow-band (~1 eV) spectra from X-ray fluorescence emission detection at the $K_{\beta}^{1,3}$ line maximum (8265.7 eV) corrected for self-absorption. K-edge energies mentioned in the text were determined at half-height (50 % level) of the normalized spectra in the main panel. Main-edge rise background subtraction from pre-edge spectra in the inset yielded the ctv spectra shown in Figure S10A.

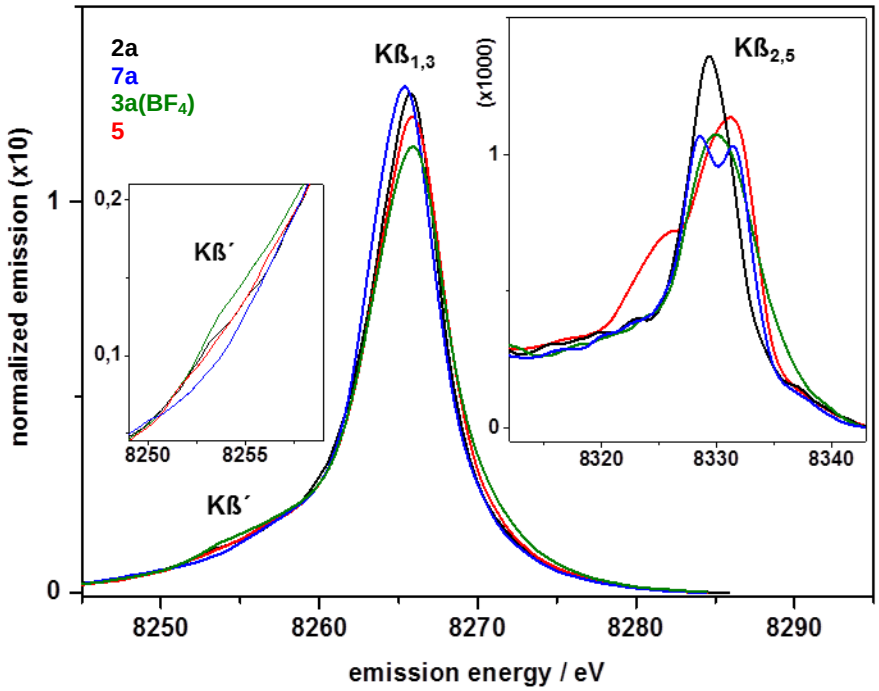

Figure S13 Kß X-ray emission spectra of Ni compounds**.** Main panel: Kß main line spectra. Left inset: Kß´ features in magnification. Right inset: Kß satellite line spectra. Main line spectra were normalized to unity area in a 8245-8345 eV energy range after setting the spectra to zero level at 8345 eV for comparison. $Kß^{2,5}$ spectra were smoothed by adjacent averaging over 5 data points (1.75 eV) for display and normalized according to the main line spectra. $Kß^{1,3}$-tail background subtraction from $Kß^{2,5}$ spectra yielded the vtc spectra shown in Figure S10B. The apparently smallest Kß´ feature for **7a** likely resulted from the spin-1/2 Ni(I) configuration (M = 2) of the tetrahedral site and shifts to lower energies of the decay transitions underlying the Kß´ multiplet features.

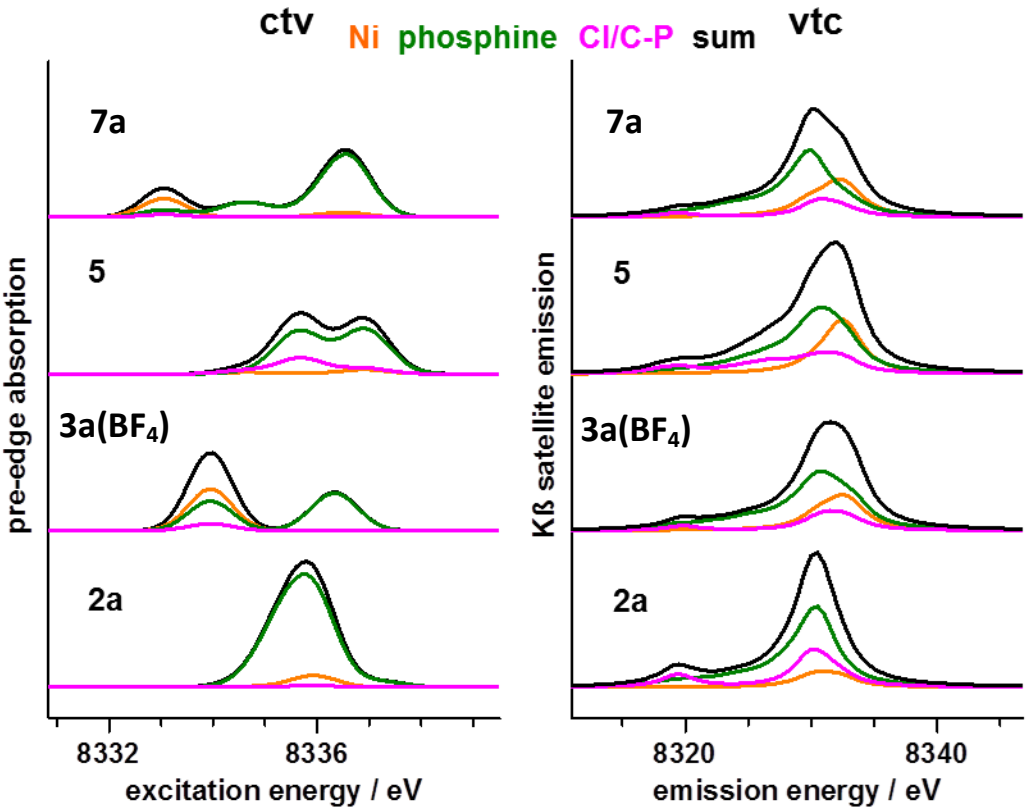

Figure S14 Nickel and ligand characters of ctv and vtc electronic transitions. (Left) ctv excitation. (Right) vtc decay. Data correspond to BP86/ TZVP single-point calculations on XRD structures. Metal and ligand characters of target (ctv) or source (vtc) MOs for calculated transitions in the spectra (sum) are color-coded as indicated (phosphine = whole ligand except other given species; Cl^- not present in **5** and replaced by a C-P group).

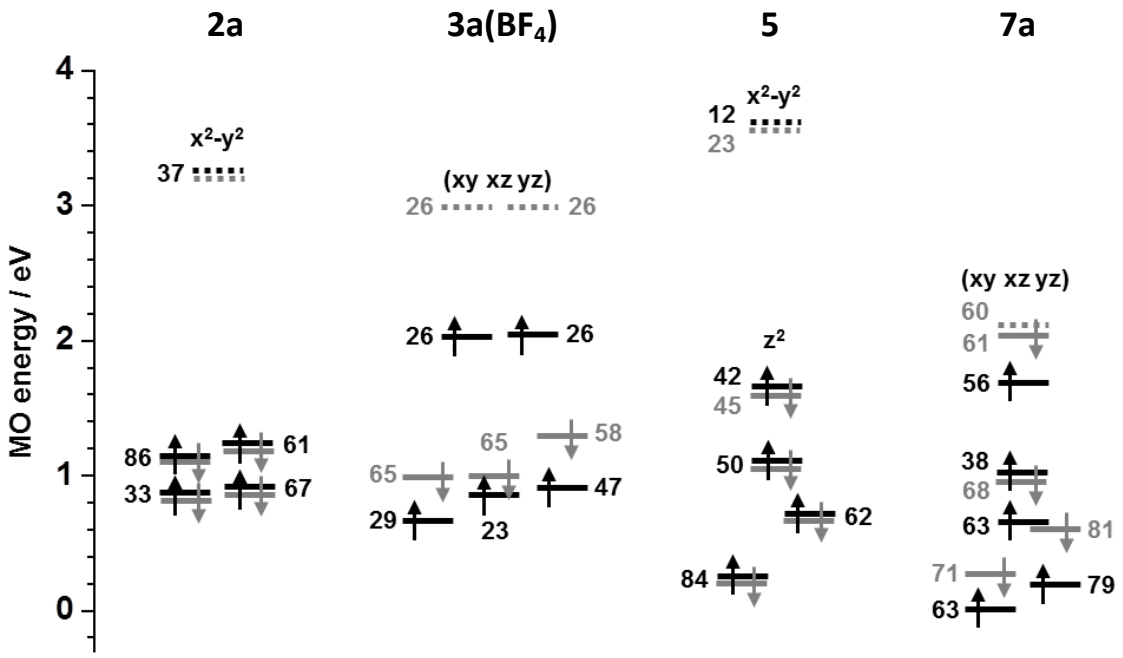

Figure S15 Ni(d) orbital degeneracy. Shown energy levels correspond to MOs with highest Ni(d) characters from single-point DFT calculations on crystal structures; numbers represent Ni(d) character of MOs in %); black/grey bars and arrows denote occupied α/ß-spin MOs; unoccupied MOs are shown as dotted bars; selected dominant specific Ni(d) characters are indicated (mixed characters in parenthesis).

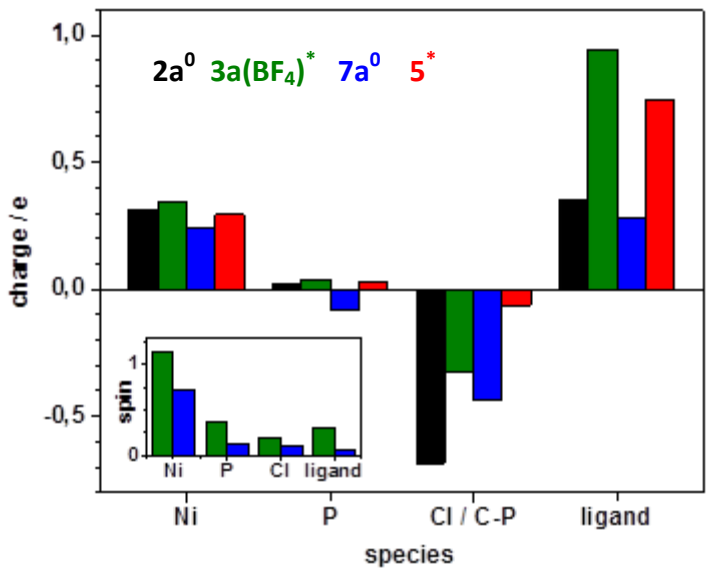

Figure S16 Charge and spin density distribution. Data represent Hirshfeld charges (CM5) and spin densities on indicated species (C-P ligand only present in **5;** ligand = remaining ligand atoms excluding P, Cl, or C-P atoms) from single-point BP86/TZVP calculations on XRD structures (complex charges for the compounds are indicated). The Si atom in **5** carries significant charge (0.17), which is summed in the ligand charge here.

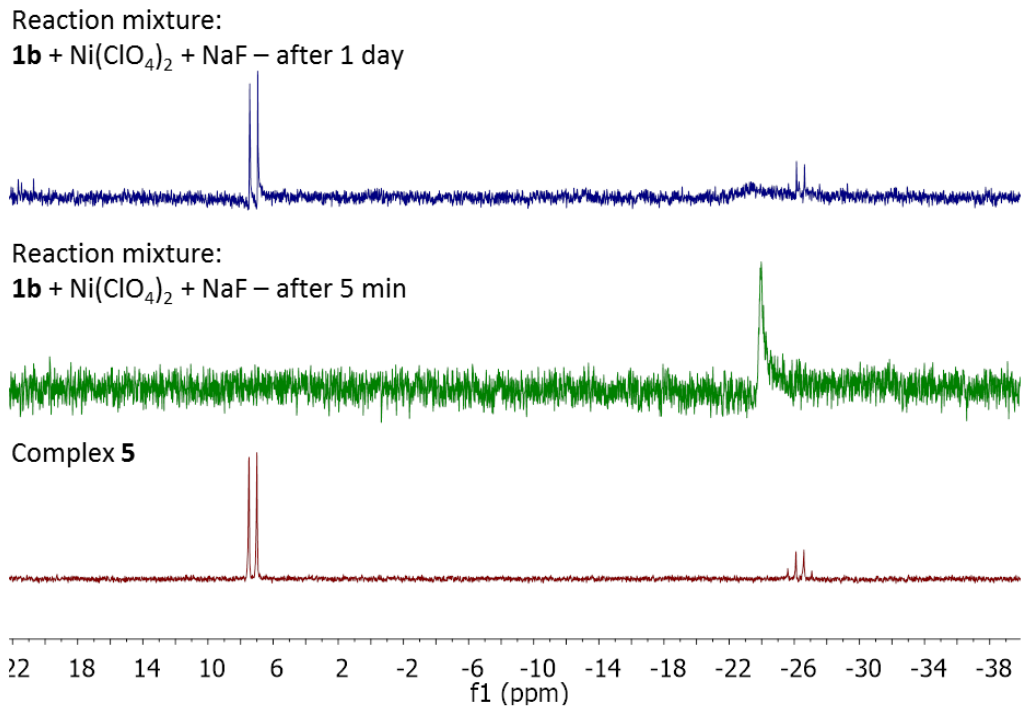

Figure S17 ^{31}P NMR spectra of complex **5** (red line), the reaction mixture of compound **1b** with $Ni(ClO_4)_2$ with NaF after 5 min (green line) and the reaction mixture of compound **1b** with $Ni(ClO_4)_2$ with NaF after 1 day (blue line) in MeCN-d_3.

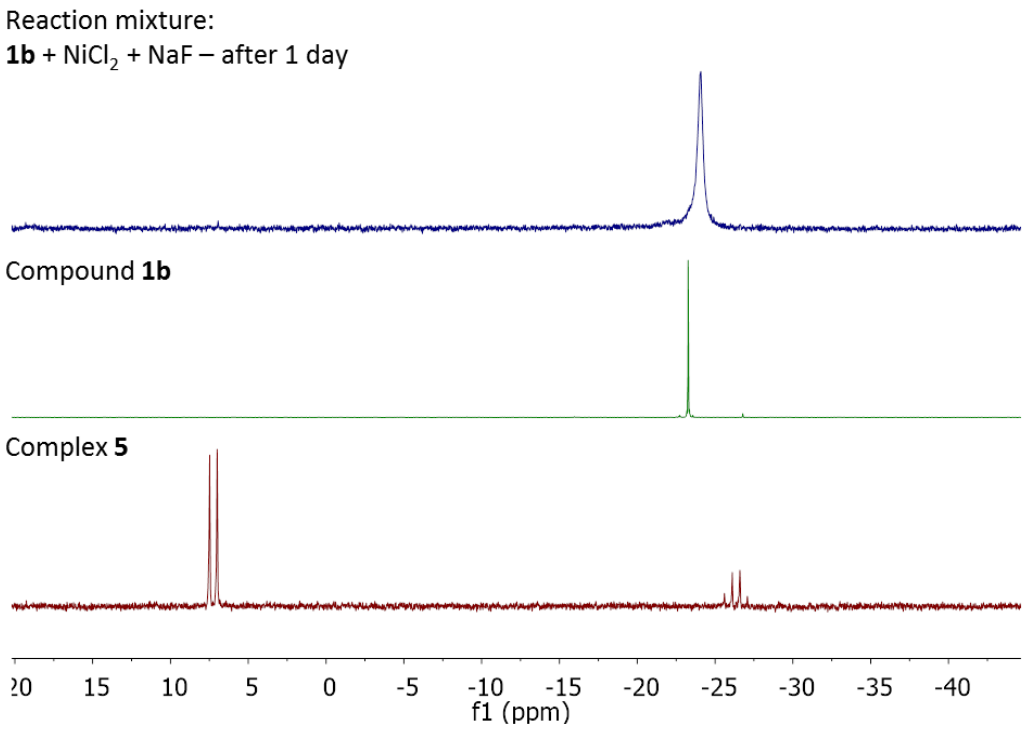

Figure S18 ^{31}P NMR spectra of complex **5** (red line), compound **1b** (green line) and the reaction mixture of compound **1b** with $NiCl_2$ with NaF after 1 day (blue line) in MeCN-d_3.

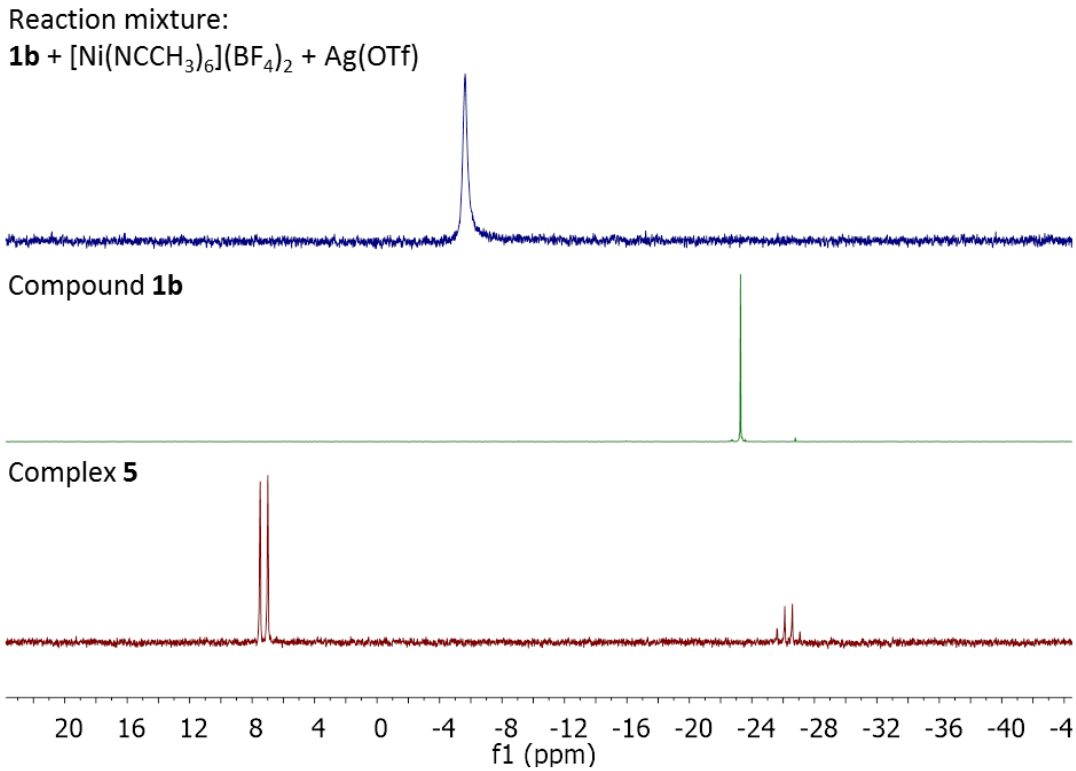

Figure S19 ^{31}P NMR spectra of complex **5** (red line), compound **1b** (green line) and the reaction mixture of compound **1b** with $[Ni(CH_3CN)_6](BF_4)_2$ with Ag(OTf) (blue line) in MeCN-d_3.

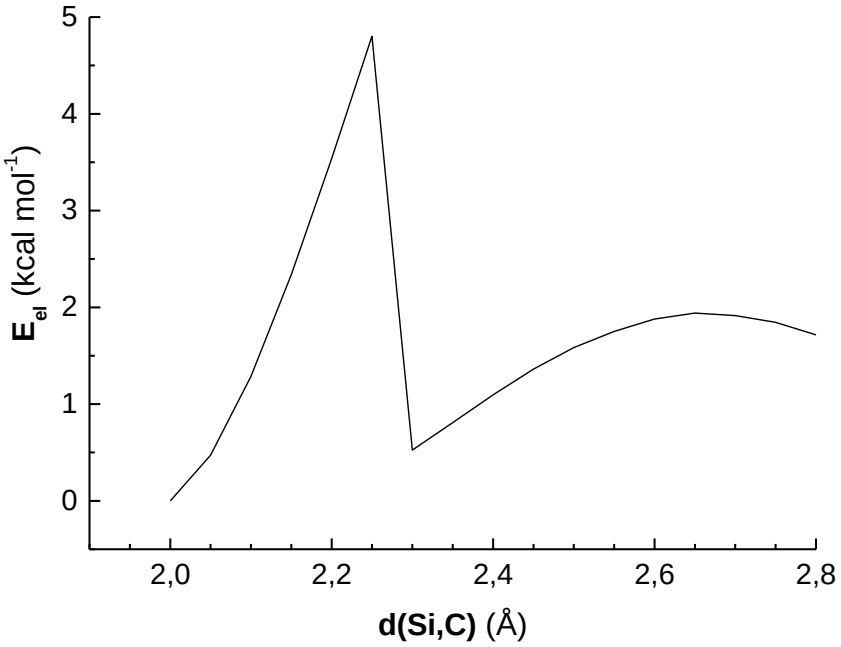

Figure S20 Relaxed surface scan for Si-C bond cleavage in the coordination complex of Triphos^{Si} to two Ni^{2+} cations after nucleophilic attack at Si by F^-. The figure demonstrates that the Si-C bond breaks at 2.3 Å leading to a slightly larger change of the internal coordinates than at other steps of the scan. The figure additionally indicates that an activation energy of only 5 kcal/mol is required for final Si-C bond cleavage after nucleophilic attack at Si has taken place.

Table S1 EXAFS fit parameters and nickel-ligand bond lengths.[a]

compound	N [per Ni ion] / R [Å] / 2σ² x10³ [Å²]		R_F [%]
	Ni-P (-C)	Ni-Cl	
2a	2 / 2.16 [2.14] / 5[#]	2 / 2.20 [2.18] / 5[#]	8.5
3a(BF_4)	3 / 2.24 [2.25] / 7	1 / 2.16 [2.16] / 2*	6.7
5	1 / 2.15 [2.13 / 2.18, 2.51] / 2* 2 / 2.23 [2.22 / 2.26, 2.40] / 7 1 / 2.32 [2.31 / 2.35, 2.36] / 2* (1 / 2.07 [2.06 / 2.01, 2.05] / 2*)		9.8
7a	3 / 2.19 [2.23] / 7	1 / 2.25 [2.26] / 2*	7.2

[a]Fit parameters are for EXAFS spectra in Fig. S8. *N*, coordination number; *R*, interatomic distance; 2σ², Debye-Waller factor; R_F, fit error sum calculated for reduced distances of 1-3 Å. *Parameters that were fixed in the simulations, [#]Debye-Waller factors were restraint to the same value for Ni-P and Ni-Cl shells, coordination numbers were fixed to the crystallographic values. Bond lengths from crystal structures / and for **5** from DFT for BP86 functional and M = 1, M = 3 spin states (for geometry-optimized structures) are given in brackets. The fits contained additional longer Ni-C/Si shells: **2a**, (C) 2 / 3.38 [3.46] / 5*; **3a**(BF_4), (C) 2 / 3.38 [3.39] / 5*; **5**, (C) 2 / 3.38 [3.33] / 5* and (Si) 1 / 3.54 [3.48] / 5*; **7a**, 2 / 3.27 [3.30] / 5*. The splitting of the first-sphere distances into several shells is tentative according to the distance resolution limit of ~0.1 Å for the given *k*-range, but results in bond lengths in good agreement with the crystallographic data.

Table S2 Molecular energies for different spin states.[a]

compound	functional	multiplicity[b]	method[c]	cycles[d]	energy / eV	ΔE / eV	preferred[f]
5	BP86	1	sp	23	-141895.72	1.99	ls-Ni(II) (1.97 eV)
		3		123	-141893.73		
		1	go	27	-141895.91	-	
		3		-[e]	-		
7a	BP86	2	sp	298	-124612.75	(-0.32)	Ni(I) (1.58 eV)
		2	go	82	-124613.07		
3a(BF_4)	BP86	1	sp	316	-124606.85	-0.87	hs-Ni(II) (3.08 eV)
		3		35	-124607.72		
2a	BP86	1	sp	24	-137137.34	1.87	ls-Ni(II) (2.04 eV)
		3		501	-137135.47		
		1	go	23	-137138.13	0.36	
		3		67	-137137.77		

[a]Data for the annotated nickel complexes for DFT calculations (BP86/TZVP). [b]Spin multiplicity (M = 2S + 1); [c]method: sp = single-point calculation using XRD coordinates, og = gas-phase geometry optimization for indicated spin states prior to energy calculation; [d]cycles needed to reach electronic structure convergence; [e]geometry did not converge to an energetic minimum; [f]preferred spin state (hs = high-spin, ls = low spin) and nickel redox state according to energy differences (ΔE) and convergence cycle numbers (in parenthesis: ΔE for **7a** is for XRD vs. relaxed structures of the M = 2 spin state), as well as (for α-spin MOs) HOMO – LUMO energy differences for the relevant spin state (in parenthesis).

Table S3 Crystal Data and Refinement Details for the Crystal Structure Analyses of Compounds **3a(BF_4)** and **3b(ClO_4)**.

	3b(ClO_4)	**3a(BF_4)**
Empirical formula	$C_{40}H_{39}Cl_2O_4NiP_3Si$	$C_{41}H_{39}ClBF_4NiP_3$
Formula weight	840.01	804.13
Temperature/K	170	293.15
Crystal system	cubic	cubic
Space group	F-43c	Fd-3
***a*/Å**	33.108(3)	33.558(2)
***b*/Å**	33.108(3)	33.558(2)
***c*/Å**	33.108(3)	33.558(2)
***α*/°**	90	90
***β*/°**	90	90
***γ*/°**	90	90
***Volume*/Å^3**	36291(6)	37790(4)
Z	32	32
ρ_{calc}g/cm^3	1.230	1.133
μ/mm^{-1}	0.713	0.609
F(000)	14016.0	13319.0
Crystal size/mm^3	0.07 x 0.05 x 0.030	0.23 x 0.19 x 0.16
Radiation	MoK_α (λ = 0.71073)	MoK_α (λ = 0.71073)
2Θ range for data collection/°	4.26 to 50.38	3.44 to 48.22
Index ranges	-39 ≤ h ≤ 39, --39 ≤ k ≤ 39, -39 ≤ l ≤ 39	-37 ≤ h ≤ 38, -38 ≤ k ≤ 38, -38 ≤ l ≤ 38
Reflections collected	61209	52558
Independent reflections	2683 [R_{int} = 0.2515, R_{sigma} = 0.0779]	7465 [R_{int} = 0.1108, R_{sigma} = 0.0821]
Data/restraints/ parameters	2683/0/144	7465/0/461
[a]Goodness-of-fit on F^2	0.923	0.0675
[b,c]Final R indexes [I≥2σ (I)]	R_1 = 0.0830, wR_2 = 0.22565	R_1 = 0.0401, wR_2 = 0.0890
Final R indexes [all data]	R_1 = 0.1110, wR_2 = 0.2451	R_1 = 0.0946, wR_2 = 0.0984
Largest diff. peak/hole/ e Å^{-3}	0.76/-0.91	0.307/-0.194
Flack parameter	1.01(6)	-
CCDC reference	1486087	1486084

[a]$S = \{\Sigma[w(F_o^2 - F_c^2)^2]/(n - p)\}^{0.5}$; n = no. of reflections; p = no. of parameters. [b] $R_1 = \Sigma ||Fo| - |Fc|| / \Sigma |Fo|$. [c] $wR_2 = \{ \Sigma [w(F_o^2 - F_c^2)^2]/(\Sigma[w(F_o^2)^2]\}^{0.5}$.

Table S4 Crystal Data and Refinement Details for the Crystal Structure Analyses of Compounds **4**, **5** and **7a**.

	4	**5**	**7a**
Empirical formula	$C_{47}H_{49}B_2F_8N_3NiP_3$	$C_{50}H_{54}BF_4NNiP_4Si$	$C_{41}H_{39}ClNiP_3$
Formula weight	980.18	1026.54	718.79
Temperature/K	105.10(14)	104.7(10)	293(2)
Crystal system	monoclinic	monoclinic	orthorhombic
Space group	$P2_1/c$	$P2_1/c$	$Pna2_1$
***a*/Å**	20.7166(5)	10.33005(10)	20.70(2)
***b*/Å**	12.4767(3)	20.6239(2)	10.259(11)
***c*/Å**	20.5881(3)	23.6859(2)	16.853(16)
***α*/°**	90	90	90
***β*/°**	109.315(2)	90.01(2)	90
***γ*/°**	90	90	90
***Volume*/Å^3**	5021.99(19)	5046.20(9)	3579(6)
Z	4	4	4
ρ_{calc}g/cm^3	1.2963	1.3511	1.351
μ/mm^{-1}	2.011	2.413	0.789
F(000)	2021.9	2135.3	1500.0
Crystal size/mm^3	0.33 x 0.26 x 0.15	0.14 x 0.11 x 0.10	0.15 x 0.11 x 0.08
Radiation	Cu Kα (λ=1.54184)	CuK_α (λ = 1.54184)	MoK_α (λ = 0.71073)
2Θ range for data collection/°	8.4 to 148.2	8.56 to 148.5	4.4 to 50.0
Index ranges	-17 ≤ h ≤ 24, -9 ≤ k ≤ 15, -25 ≤ l ≤ 16	-12 ≤ h ≤ 11, -23 ≤ k ≤ 25, -28 ≤ l ≤ 29	-30 ≤ h ≤ 33, -13 ≤ k ≤ 14, -24 ≤ l ≤ 28
Reflections collected	13488	26336	29335
Independent reflections	7884 [R_{int} = 0.0178, R_{sigma} = 0.0247]	9610 [R_{int} = 0.0144, R_{sigma} = 0.0141]	6292 [R_{int} = 0.1148, R_{sigma} = 0.1006]
Data/restraints/ parameters	7884/0/575	9610/10/645	6292/1/416
[a]Goodness-of-fit on F^2	1.049	1.062	1.097
[b,c]Final R indexes [I≥2σ (I)]	R_1 = 0.0463, wR_2 = 0.1227	R_1 = 0.0321, wR_2 = 0.0838	R_1 = 0.0550, wR_2 = 0.1183
Final R indexes [all data]	R_1 = 0.0499, wR_2 = 0.1272	R_1 = 0.0342, wR_2 = 0.0846	R_1 = 0.075, wR_2 = 0.1412
Largest diff. peak/hole/ e Å^{-3}	1.27/-0.87	1.105/-0.685	0.370/-0.572
Flack parameter	-	-	-0.01(2)
CCDC reference	1486081	1486082	1486083

[a]$S = \{\Sigma[w(F_o^2 - F_c^2)^2]/(n - p)\}^{0.5}$; n = no. of reflections; p = no. of parameters. [b] $R_1 = \Sigma ||Fo| - |Fc|| / \Sigma |Fo|$. [c] $wR_2 = \{ \Sigma [w(F_o^2 - F_c^2)^2]/(\Sigma[w(F_o^2)^2]\}^{0.5}$.

Table S5 Crystal Data and Refinement Details for the Crystal Structure Analyses of Compounds **7b**, **8** and **9**.

	7b	**8**	**9**
Empirical formula	$C_{40}H_{39}BrNiP_3Si$	$C_{14}H_{39}B_2Fe_8NNiP_{34}$	$C_{15}H_{51}B_2F_8NiO_6P_5$
Formula weight	779.33	577.7	714.74
Temperature/K	170(2)	108.2(6)	193(2)
Crystal system	monoclinic	Monoclinic	orthorhombic
Space group	$P2_1$	$P2_1/c$	$Pna2_1$
***a*/Å**	10.2603(18)	10.1498(3)	21.1905(6)
***b*/Å**	17.719(2)	16.0585(6)	13.5221(4)
***c*/Å**	10.385(2)	19.1814(7)	11.3801(3)
***α*/°**	90	90	90
***β*/°**	105.514(15)	121.948(2)	90
***γ*/°**	90	90	90
***Volume*/Å^3**	1819.1(6)	2652.83(16)	3260.85(15)
Z	2	4	4
ρ_{calc}g/cm^3	1.423	1.446	1.456
μ/mm^{-1}	1.824	3.891	0.913
F(000)	802	1200	1496.0
Crystal size/mm^3	0.15 x 0.11 x 0.08	0.14 x 0.11 x 0.10	0.16 x 0.14 x 0.11
Radiation	MoK_α (λ = 0.71073)	CuK_α (λ = 1.54184)	MoK_α (λ = 0.71073)
2Θ range for data collection/°	5.46 to 50	7.8 to 148.6	6.02 to 73.52
Index ranges	$-12 \le h \le 12$, $-21 \le k \le 21$, $-12 \le l \le 12$	$-12 \le h \le 12$, $-18 \le k \le 19$, $-23 \le l \le 23$	$-25 \le h \le 25$, $-16 \le k \le 18$, $-13 \le l \le 13$
Reflections collected	9961	14226	44950
Independent reflections	5979 [R_{int} = 0.048, R_{sigma} = 0.0739]	4798 [R_{int} = 0.0244, R_{sigma} = 0.0244]	5730 [R_{int} = 0.0430, R_{sigma} = 0.0233]
Data/restraints/ parameters	5979/0/416	4798/0/282	5730/1/313
[a]Goodness-of-fit on F^2	0.882	1.042	1.069
[b,c]Final R indexes [I≥2σ (I)]	R_1 = 0.0335, wR_2 = 0.0668	R_1 = 0.0460, wR_2 = 0.1200	R_1 = 0.0497, wR_2 = 0.1347
Final R indexes [all data]	R_1 = 0.0450, wR_2 = 0.0692	R_1 = 0.0510, wR_2 = 0.1244	R_1 = 0.0538 wR_2 = 0.1398
Largest diff. peak/hole/ e Å^{-3}	0.533/-0.460	1.104/-0.970	0.717/-1.078
Flack parameter	-0.013(8)	-	0.118(18)
CCDC reference	1486085	1486088	1486086

[a]$S = \{\Sigma[w(F_o^2 - F_c^2)^2]/(n - p)\}^{0.5}$; n = no. of reflections; p = no. of parameters. [b] $R_1 = \Sigma ||Fo| - |Fc|| / \Sigma |Fo|$. [c] $wR_2 = \{ \Sigma [w(F_o^2 - F_c^2)^2]/(\Sigma[w(F_o^2)^2]\}^{0.5}$.

Table S6 Cartesian coordinates [Å] of the coordination complex of Triphos^{Si} to two Ni^{2+} cations after nucleophilic attack of F^- at Si.

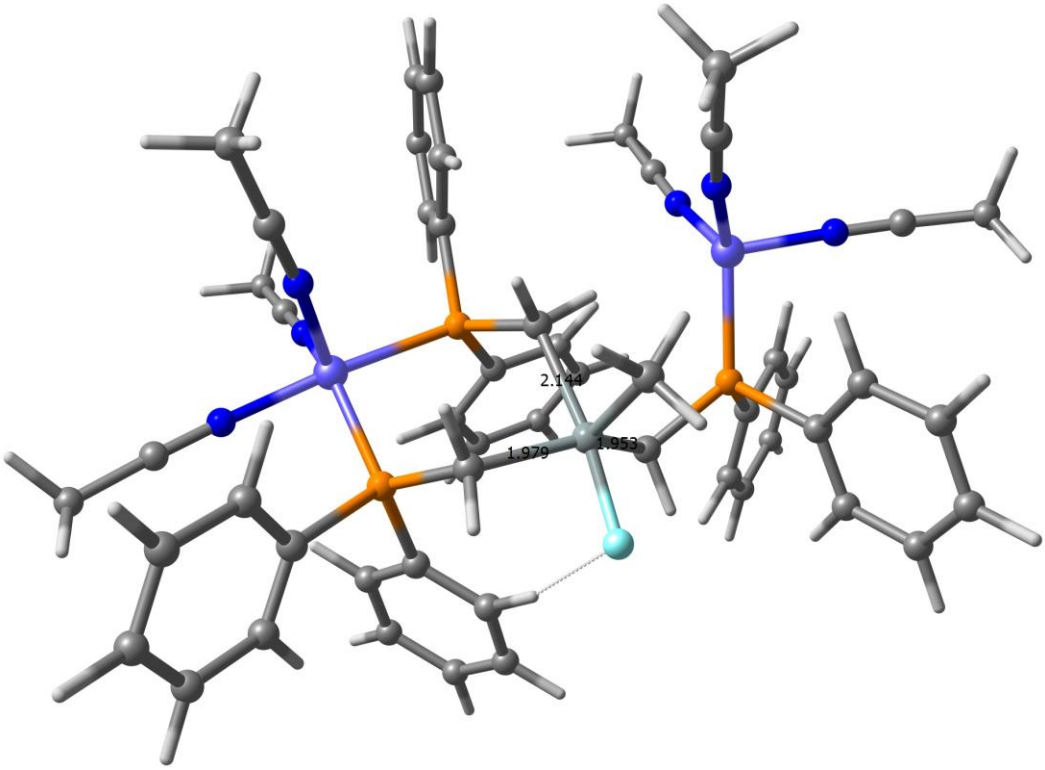

Ni	12.10496459551666	8.43441770907700	8.10201090724329
P	13.05485707612065	6.59980451736385	9.04455907795632
P	12.90902184842887	7.82083563095079	6.02858654517415
P	15.39320995354598	4.45787532395194	3.74028570059961
C	14.22724606826807	3.40084318787027	2.71933860144993
N	11.22697017879591	8.79489307405295	9.79251447136016
C	12.10837671188276	5.02262976096251	8.92824867901519
C	12.61510499689466	5.98818532936477	11.83444460993362
H	12.00660128628397	5.14048667945847	11.49853404379014
C	16.69826316591470	1.92660258018142	4.25246159919159
H	15.69882559232437	1.47530427112347	4.29651005735661
C	12.73015643586162	9.35551801116633	4.98175068618078
C	10.77082853242343	8.97493531651980	10.85503806849429
C	13.39271842884824	2.40467429153828	3.27393335762409
H	13.39739761791837	2.22316893013310	4.35569465047849
C	10.71461731744070	5.04909012264874	9.16932040906613
H	10.21870644362893	6.00621034345039	9.38160503166678
C	14.15640749877634	3.63647727477012	1.32862491664922
H	14.76998236138631	4.43875031296762	0.90059950558281
N	13.37203659064023	9.94258280228288	8.30203390717568
C	17.16429186619417	6.04317657934283	6.59212064857584
H	17.40079088289609	6.88314539804581	7.27322447555229
H	17.84872439541239	5.21022280342223	6.82802223434512
H	17.35355496673578	6.37676530607133	5.55934104568599
C	14.03037870195909	10.89766299332959	8.47170188591273
C	12.80493934673166	6.20131333661237	13.21350425737825
H	12.33967926494227	5.51687831884982	13.93392547824824
C	14.77764854626021	6.27300144114359	8.55119411806956

H	15.26013131936129	7.26881905158032	8.58034344934253
H	15.23757741903196	5.65113007473542	9.33937253356511
C	11.97910806655403	2.61107246140443	8.60210160843063
H	12.47737965291757	1.66002008640151	8.37610768025083
C	13.78290990596628	10.29601156182240	4.93222144959872
H	14.71542127681330	10.09237974803519	5.47212678662660
C	11.56444525799130	9.61139750631709	4.22385800024462
H	10.75119045925196	8.87460996681481	4.21561471991171
C	13.66775503637956	11.46785694999929	4.16596964051636
H	14.50271620652295	12.18022511967078	4.13056488965317
C	12.53253836331310	1.64920268310104	2.45753665549938
H	11.89498565084764	0.87785461870732	2.90894871028819
C	14.58214536563947	4.38219476146994	5.41654984846860
H	13.52220946425438	4.64994777074001	5.26010145612018
H	14.63090385238584	3.33565503947653	5.76424444702069
C	13.59986544485781	7.26800840551548	13.66592549471838
H	13.75878088374620	7.42364374178669	14.74045481783781
C	12.49784527200634	11.72106551488945	3.42790093534098
H	12.40943264404277	12.63445367645022	2.82667079555766
C	18.14872102460729	3.84111761185411	3.90549232992507
H	18.26293125600996	4.90872399350798	3.67968963222006
Si	15.35728996775096	5.48281398267726	6.83132825644884
N	10.54592042155972	9.13355832761169	7.26055233337595
C	14.01830942485009	7.91324700040929	11.35297519950719
H	14.49787499174509	8.58747062869606	10.63212434287393
C	11.15215864221888	5.34858087795540	3.20449840210262
H	11.39296549245440	4.99789804576499	2.19392867423304
C	19.27619884034837	3.02756165523522	4.11618583752470
H	20.28207260639696	3.46510006871407	4.06622034596571
C	17.82324307614478	1.11089566687346	4.45808396960393
H	17.68851159571481	0.04308802201210	4.67250454971357
C	10.59826505114467	2.63907944423171	8.85737937211932
H	10.01382424421813	1.71075970817630	8.83223851071546
C	19.11639856701282	1.65964107923185	4.39373821730593
H	19.99425582493445	1.02287479654910	4.56007458196293
C	13.29870620451202	2.88127134252354	0.51001479365559
H	13.26147118370927	3.07801761064278	-0.56984308248438
C	11.45050083804205	10.78252516077146	3.45311253628814
H	10.54151385518503	10.95883955290025	2.86253141332258
C	11.75851631306259	6.64548114777171	5.18290589478427
C	13.22150786877630	6.84098081522441	10.88761892605306
C	12.74166232543948	3.79396592814727	8.63816062226024
H	13.82146152259659	3.75374040820987	8.42997398725905
C	14.59784878781983	7.23041953158574	5.84828918225068
H	14.81267569603890	7.05896431497822	4.75344318387759
H	15.25191288051160	8.05931884894500	6.18340905662090
C	16.84706312481539	3.30332167291796	3.97908787145585
C	12.03774914448415	6.21523932876152	3.86555608938649
H	12.96233142277626	6.52880295545941	3.36388055728842
C	10.58883659096799	6.19169186280070	5.82456970255159
H	10.38628328915173	6.50865982895988	6.85284604303953
C	14.20788253360595	8.12403202580387	12.72774431751495
H	14.84010437459291	8.95352849918614	13.07060177885858
C	12.48548708226688	1.88068803542718	1.07172619159718
H	11.81524902767019	1.28915620393924	0.43511915742519
C	9.96455688588032	3.86336042270448	9.14292246142442
H	8.88586448200695	3.89291268995392	9.34199929422668

C	9.98120605799769	4.90708599698913	3.84728910761768
H	9.29544067495837	4.22471247359871	3.32954971391400
C	10.25486805511691	9.15579499750135	12.20311448595743
H	9.24514977373061	8.71822629060621	12.29474710612323
H	10.92780429395605	8.64682947398662	12.91750547435120
H	10.20016957594736	10.22783594257742	12.46181776328981
C	9.70335966564553	5.32549921356848	5.15879707933931
H	8.80321466713736	4.96760941177253	5.67366078669877
C	14.84330609639045	12.08946000171313	8.67264958981372
H	14.87313151537477	12.69130811507009	7.74652289201276
H	14.41933839463187	12.71249675860821	9.48047047034516
H	15.87684534477953	11.81466317112852	8.94893055123819
C	9.57138867780419	9.61864159088414	6.82654055326863
C	8.37091192170780	10.22676822866269	6.27349651433853
H	7.81309109344967	10.76434186347869	7.06095419125270
H	8.64328307328802	10.94752938187565	5.48135114848991
H	7.70903581132562	9.45597991678553	5.83838870819957
Ni	15.98537871516547	6.32453920798542	2.67202373293929
C	18.58267457152724	4.35958742976929	-0.44940224491031
H	19.28973557011999	5.06938741847085	-0.91579385299357
H	19.16433394109918	3.56709247881723	0.05639848558381
H	17.98447928849103	3.88997899995044	-1.25131093809559
C	19.18452981198076	9.15415470941035	4.06886892138093
H	20.03777270989834	9.04974259851910	3.37318957957830
H	18.87082366668523	10.21467231570269	4.06761966887307
H	19.53864280029892	8.89773527103802	5.08482619109242
C	18.09011071294914	8.27942159786180	3.67002220346520
N	17.22861131334471	7.54096685897402	3.35001597990741
C	17.72013363163124	5.03691719846652	0.50874569729721
N	17.02697307761726	5.55022122639035	1.30877215305289
C	12.97454978588651	8.69911373171898	0.32031810837747
H	12.23821615150695	9.20036029666163	0.97522314826849
H	13.51282890788789	9.47808854958270	-0.25088584214341
H	12.42735463088086	8.06005299654902	-0.39681184007608
C	13.90055209854370	7.90950175244857	1.11902530717853
N	14.65711469815871	7.27910113247029	1.76720000613648
F	15.70017572114529	4.02724773671993	7.72369545183299